IV.A.1d Reversible Hydrogen Storage Materials – Structure, Chemistry, and Electronic Structure

Ian M. Robertson (Primary Contact),
Duane D. Johnson, Dennis D. Graham,
Nikolai Zarkevich
University of Illinois at Urbana-Champaign (UIUC)
Department of Materials Science and Engineering
1304 West Green Street
Urbana, IL 61801
Phone: (217) 333-1440; Fax: (217) 333-2736
E-mail: ianr@illinois.edu

DOE Technology Development Manager:
Ned Stetson
Phone: (202) 586-9995; Fax: (202) 586-9811
E-mail: Ned.Stetson@ee.doe.gov

DOE Project Officer: Paul Bakke
Phone: (303) 275-4916; Fax: (303) 275-4753
E-mail: Paul.Bakke@go.doe.gov

Contract Number: DE FC36-05GO15064

Project Start Date: March 1, 2005
Project End Date: February 26, 2010

Objectives

The main focus of UIUC within the Metal Hydride Center of Excellence (MHCoE) is to:

- Advance the understanding of the microstructural and modeling characteristics of complex hydrides.
- Provide feedback and knowledge to partners within MHCoE framework.
- Provide more reliable theoretical methods to assess hydrogen-storage materials, including key issues affecting materials under study.

Technical Barriers

This project addresses the following technical barriers from the Storage section of the Hydrogen, Fuel Cells and Infrastructure Technologies Program Multi-Year Research, Development and Demonstration Plan:

(A) System Weight and Volume

(E) Charging/Discharging Rates

Technical Targets

Our characterization and theoretical tools are general and can be used with many materials above and beyond complex hydride materials. The following is a sample of the results that we have obtained with our tools.

- Demonstrated ability to quantify efficacy of ball-milling and mixing for dispersion of catalysts for MgH_2, $Ca(BH_4)_2/CaB_6$, and Ti-doped $NaAlH_4$.
- Detailed issues involving reversibility and intermediate amorphous materials in $Ca(BH_4)_2$.
- Developed new theoretical method for accurate prediction of reaction enthalpies in molecular solids. This advance eliminates previous limitations of this method.
- Quantified size and confinement effects on Mg/MgH_2 supported nanoparticles and their adsorption properties.

Accomplishments

- Modeled complex hydride systems.
- Applied reaction enthalpy prediction to systems of interest, and used these accurate predictions to generate van't Hoff plots.
- Helped understand intermediate phases generated during charging/discharging cycles and the role they have in system reversibility.
- Completed joint experiment and theory analysis of temperature dependent X-ray diffraction (XRD) analysis of $LiBH_4$.

✧ ✧ ✧ ✧ ✧

Introduction

Our work at UIUC focuses on resolving issues within current hydrogen storage materials using a combination of electronic structure calculations and chemical analysis. We tie together theoretical understanding of electronic, enthalpic, thermodynamic, and surface effects that influence performance of storage materials with microchemical and microstructural experimental analysis. These efforts are coordinated with those of other MHCoE partners.

We established partnerships in Fiscal Year 2007 with the following groups: Sandia National Laboratories (SNL), HRL, University of Pittsburgh (Pitt), Georgia Institute of Technology (Georgia Tech), University of Hawaii, and University of Nevada, Reno.

Approach

We employ state-of-the-art characterization tools to investigate the microstructural and microchemical changes that occur in candidate material systems during the uptake and release of hydrogen. This investigation provides fundamental insight to the processes governing hydrogen uptake and release. The characterization is coupled with first-principles, electronic-structure and thermodynamic theoretical techniques to predict and assess meta-stable and stable phases, as well as surface effects that can poison or limit kinetics. Electronic-structure and thermodynamic calculations are used to enhance the understanding of MHCoE experimental characterization results on candidate systems. The theoretical work at UIUC is coordinated closely with MHCoE theory partners, as well as experimental efforts.

Results

Theory Results

Universal Behavior of Transition-Metal Nanoparticles Core-Shell Preferences Core-shell nanoparticles are ubiquitous in catalysis, fuel cells, and bio-related applications due to control of size, performance, biocompatibility, and cost. We investigated segregation energies of 132 binary systems using density functional theory (DFT) and determine core-shell preferences, which agree with available observations. Segregation and *composition-averaged* segregation energies were determined from $(A_6)B_{32}$ and $(B_6)A_{32}$ core-shell (38-atom) particles, where parentheses indicate core species. There were no qualitative changes in results from varying sized particles. From the segregation energies, we showed that core-shell preferences are described by two simple factors: *cohesive energy* (related to vapor pressure) and *atomic size* (Wigner-Seitz radius). As shown in Figure 1, arranging the segregation energies of core-shell nanoparticles according to cohesive energy and atomic size of the elements yields a fully ordered array that agrees with all known observations of core-shell preference. No other parameters lead to proper prediction and clear pattern for the core-shell preference. A paper on this topic was submitted 30 June 2008.

We provided a universal description of core-shell preference via tight-binding theory that quantitatively reproduces the DFT results and reveals the electronic origins for core-shell behavior. The tight-binding had no adjustable parameters, depending only on the coordination number of the atom and the number of atoms exchanged between the core and shell. There is quantitative agreement with the DFT results. Notably, in highly distorted cases, such as AuCo and AgCo, the DFT configuration was used to obtain the numerical result for the tight-binding based upon the actual coordination number.

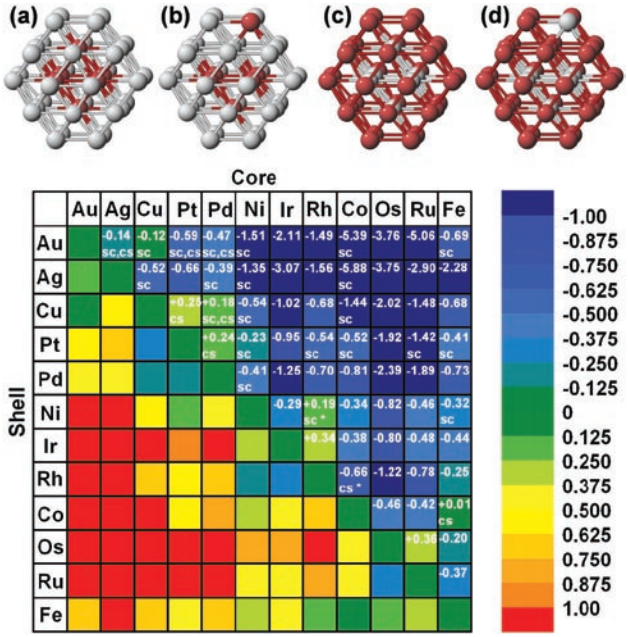

FIGURE 1. (a-d) The $(A_6)B_{32}$ and $(B_6)A_{32}$ core-shell (38-atom) particles (A atoms are red, B atoms are grey) used to determine the segregation energies in *Figure 1e.* Clusters (a) and (b) yield the segregation energy of core A going to shell B at composition c_0, i.e. $\Delta_{AB}^{c_0}$, whereas clusters (c) and (d) yield the segregation energy of core B going to shell A at composition $1–c_0$, i.e., $\Delta_{AB}^{1-c_0}$. These two segregation DFT energies $\bar{\Delta}_{AB}$ provide the *"average" segregation energy.* For Cu-Au, e.g., $\Delta_{AB}^{c_0} = -1.27\,eV$ and $\Delta_{AB}^{1-c_0} = +1.03\,eV$, so that $\bar{\Delta}_{AB} = -0.12\,eV$ slightly favoring Cu in the core, as observed, as listed Figure 1e. (e) Matrix of DFT-PW91 $\bar{\Delta}_{AB}$ for core-shell nanoparticles with 12 late-transition metals (132 binaries), color-coded with dark blue (red) as favorable in core (shell) for the transition metal listed on the top. Segregation energy values (in eV) for the upper half triangular matrix are listed, along with the available observed core-shell pattern (as reviewed in Ref. 1) labeled by sc (cs) to indicate preference of the metal on the left is in the shell (core) and the metal on the top is in the core (shell). For some pairs, both patterns are observed. For CoRh and NiRh, the asterisk means the observed preference is different from the DFT calculations, but explained by organic ligands used within experiment. Data in lower half matrix are same magnitude but opposite sign.

We are completing a paper on van't Hoff plot prediction with Sholl and Alapati.

The Structural Database (see http://data.mse.uiuc.edu) As part of DOE/BES DEFG02-03ER46026 for alloys and later extended through MHCoE (DEFC36-05GO15064) for hydrogen-storage materials, we developed an electronic, searchable database of first-principles DFT results to store, search, and utilize results from partners, as was done by UIUC, as well as CMU/Georgia Tech in their thermodynamic linear-search for reaction paths. Information that is available includes energies, structures, comments regarding k-points, types of DFT, etc., in order to reproduce or utilize

results reliably. The database has over 5,000 alloys, and hundreds of H-storage compounds and gases. In 2009, we are cooperating with the GridChem project at the National Center for Supercomputing Applications to extend the database to open-access, not just DOE, so that the project has higher impact.

In order to test the Structural Database and continue increasing content within the database, we have spent a limited time testing rapid estimates of phase transformation. We focused on metallic alloys, rather than hydride systems, as the estimates of transition temperatures can be readily compared against observed transition temperatures. However, the rapid estimates will be applicable to hydride systems, when the restrictions of the theory are fully understood. This work was done in cooperation with a DOE/Basic Energy Sciences alloy theory grant (D.D. Johnson), which supports the structural database enhancements within alloy theory context, as acknowledged.

We have finalized our theoretical description of general molecular solids, which form the basis of many of the studied hydrogen-storage materials, to provide an accurate predictive capability in systems of interest. In short, we have shown how to include the anharmonic vibrational (constrained molecular rotational) modes along with the usual internal molecular harmonic modes (found via standard phonon calculations) to predict quantitatively the enthalpies of reaction in critical systems (see Figure 2 for destabilized $LiBH_4$ reaction). The approach was shown to apply to solid-solid and solid-metal transformations.

We are finalizing (with D. Sholl at Georgia Tech) how the above approach can be used to determine quantitatively the van't Hoff plots usually determined by experiment.

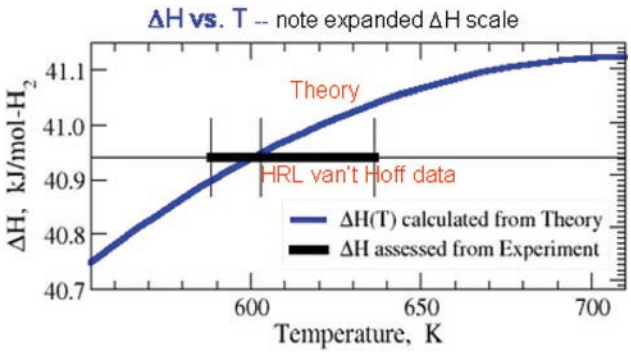

FIGURE 2. Enthalpy (in kJ/mol-H_0) of destabilized $LiBH_4$ + MgH_2 H-storage reaction (Phys. Rev. Letts. 2008) calculated from new, density-functional theory estimate that includes anharmonic rotational modes within molecular solids using simple mode-counting, along with standard harmonic (phonon) vibrational contributions. Theory calculates reaction enthalpy of 41 kJ/mol-H_2 compared to 41 kJ/mol-H_2 from HRL (J. Vajo). Typically, enthalpy estimates have been 20-100% in error due to neglect of non-harmonic vibrational modes.

Experimental Results

$Ca(BH_4)_2$ Materials

We have observed the behavior of $RuCl_3$ and Ti in $Ca(BH_4)_2$-based materials generated at SNL. In this material, $RuCl_3$ and $TiCl_3$ are added and ball-milled according to accepted principles for hydrogen storage materials. This material is reported to have approximately 6 wt% storage capacity.

We observe, after cycling, segregation of $RuCl_3$, but not $TiCl_3$ in both dehydrided and hydrided doped forms of $Ca(BH_4)_2$, as shown in results from energy dispersive spectroscopy (Figure 3). This observation suggests that the $TiCl_3$ effectively dissolves within the $Ca(BH_4)_2$ material, but not $RuCl_3$. This raises the interesting question about the processes by which these catalyst particles function.

The partial electronic density of states for CaB_6 and $Ca(BH_4)_2$ has been calculated using the Vienna ab initio simulation package for identification against the possible products of the borohydride dehydriding reaction. The energy losses after the edge onset are generally very rich in boron. These complex energy losses correspond in a qualitative fashion to the unfilled density of states in the conduction band resulting from s → p transitions. Therefore, computing the partial p-orbital density of states for boron indicates that there is a difference in the boron bonding between the B_6^{2-} unit and the BH_4^- unit. This difference, when blurred out to represent the resolution achievable in transmission electron microscopy (TEM) electron energy loss spectra, appears

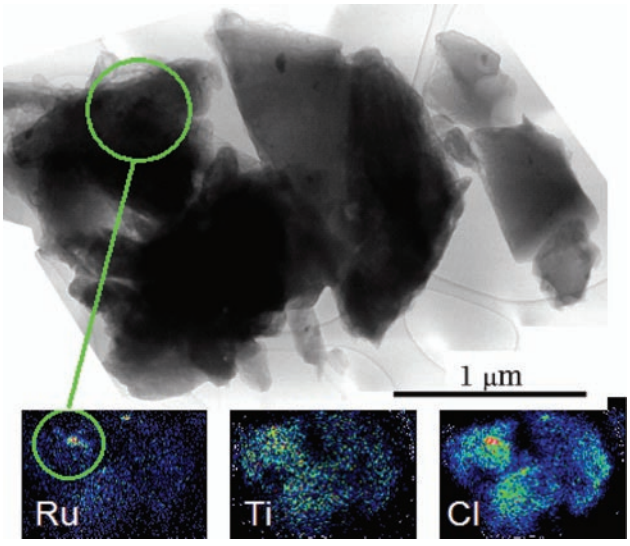

FIGURE 3. Energy dispersive mapping of elemental distribution of Ru, Ti and Cl within 3 wt% $RuCl_3$ and $TiCl_3$ doped, dehydrided, 2 cycle $Ca(BH_4)_2$. The image clearly shows that Ti is evenly distributed throughout the structure, whereas there still remain regions of $RuCl_3$ (circled) even after cycling.

to retain a discernable difference and may represent a way to distinguish, on the microscale, the chemical difference between the two materials. However, in the process of obtaining the spectra for Ru segregation, it was noted that the $Ca(BH_4)_2$ material was slowly degrading, even under "low-dose" scanning transmission electron microscope (STEM) conditions. After analysis by energy dispersive spectroscopy in STEM mode for an extended period, a $Ca(BH_4)_2$ particle was markedly degraded. This beam sensitivity precludes a detailed investigation to probe for chemical differences.

The beam degradation takes the form of H_2 bubbles in hydrided $Ca(BH_4)_2$. These bubbles grow with continued exposure to the electron beam; the mechanism of formation of these bubbles is currently being investigated. The threshold dose for bubble formation was approximately 0.1 C/cm^2, which is similar to prior calculations reporting a beam damage threshold in $NaAlH_4$ of ~0.05 C/cm^2 [1].

It has been reported by SNL (our partner in the analysis) that the dehydrided form of the $Ca(BH_4)_2$ contains a significant weight fraction that appears amorphous in X-ray diffraction patterns. Analysis of this phase is important as it represents the end-point of the reversible $Ca(BH_4)_2$ storage reaction. Electron diffraction from this intermediate phase shows a featureless pattern which is consistent with it being amorphous. Interestingly, in comparison to the hydride phase this intermediate phase was less sensitive to degradation by the electron beam and it was possible to use the electron beam to probe for elemental redistribution during the dehydring reaction. Utilizing a point-by-point electron energy loss spectroscopy (EELS) spectrum scan, we show there is no statistically significant chemical variation between points in the dehydrided material (see Figure 4). The hydrided material was also observed as a test of the technique and a 2:1 ratio of B:Ca was obtained. These result suggests that if the $Ca(BH_4)_2$ is indeed dehydriding to the dodecaborane intermediate as suggested by Hwang et al. [2], it must do so without major elemental redistribution.

Analysis of the XRD patterns indicate that the 2 CaH_2 + CaB_6 materials fabricated at SNL contained significant amounts of CaO. However, the stoichiometry of the material remains 2:1 CaH_2/CaB_6, indicating that the materials have oxidized in equal amounts. Since the free energy for oxidation of the two materials is nearly equal for the temperature range of investigation (from room temperature to ~400°C), this does not rule out oxidation of the starting materials.

Grain size analysis of cycled and as-milled CaB_6/CaH_2 mixtures has been completed. Although the materials do not uptake and release hydrogen, the grain size appears to decrease upon "cycling". This is likely due to thermal expansion causing cracking of the particulates upon heating and cooling.

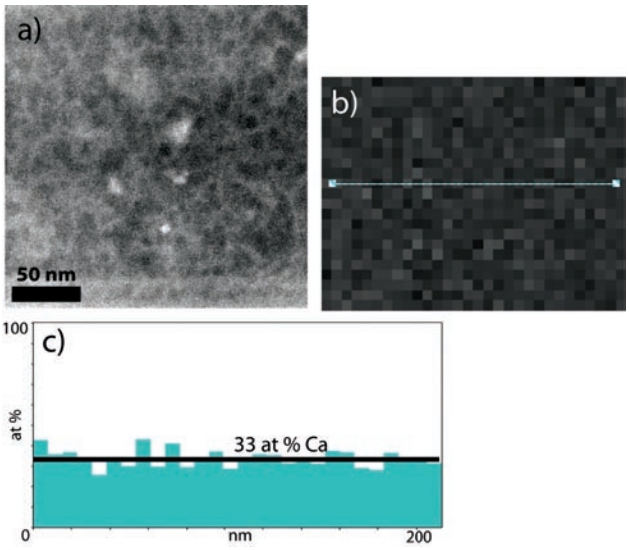

FIGURE 4. In the dehydrided $Ca(BH_4)_2$ material (dark-field image in a), STEM and EELS have been used to provide chemical information on the microscale about the intermediate phase. The normalized (0-100%) relative composition of Ca is shown in b) and this is quantified in the line scan in c) which shows the composition is stable at 2:1 B:Ca across large areas. In the experiment performed here, it is estimated that between 250 and 8,000 $Ca(BH_4)_2$ units are scattering. This constrains the maximum amount of segregation of the material and suggests that the $Ca(BH_4)_2$ is dehydriding in place.

We previously reported the formation of abnormally large crystals in a sample of CaB_6 + 2 CaH_2 + 0.04 $TiCl_3$ cycled three times. These crystals have been examined with EELS and energy dispersive X-ray spectroscopy, indicating primarily calcium and chlorine, with varying amounts of oxygen. Microdiffraction was performed on crystals to determine the crystal structure which we reported as tetragonal. However, on acquiring and analyzing additional diffraction patterns, we now believe that the structure is not tetragonal but the $CaCl_2$ orthorhombic structure.

Magnesium Hydride System

In the electron microscope, MgH_2 has been observed to have associated crystallites on the carbon grid on which the materials are placed. These satellite crystals have been identified as pure Mg by comparison of simulated and experimental diffraction patterns. The origin of these crystals is due to the electron beam sputtering material from the sample which is then re-deposited on the grid. MgH_2 has been reported as marginally stable under the electron beam, forming a hydrogen defect superstructure [3] or pure Mg [4]. However, this form of beam damage does not explain the Mg present on the grid. Loss of hydrogen from MgH_2 due to interaction with the electron beam and the subsequent formation of Mg may offer an explanation for

the failure of prior in situ TEM annealing experiments to observe the MgH_2 + Si reaction described by Vajo et al.[5]. Resolving this potential issue of damage requires the measurement of the incident beam current and the damage rate of a hydrided MgH_2 foil, which was not performed previously but is in progress.

Preliminary work has been performed on tomographic reconstruction of hydrogen storage materials and their structures. Tomography is a technique to reconstruct depth information that is missing from a static image of any material and is being applied to identify the location of catalyst particles in the matrix. Preliminary work was performed on a Ni-doped Mg/Si mixture provided by HRL and $RuCl_3$-doped $Ca(BH_4)_2$ provided by Sandia. In the Mg mixture, it was found that the Ni nodules do not have any specific preference for the surface and can be found at all depths within the crystal (Figure 5). The surface of the Ni particle was observed in high resolution STEM and found to be encased in a thin layer of Mg. The layer was confirmed as Mg (and not Ni or NiO) by EELS. This observation, if shown to be general, raises the interesting question about how these particles serve as catalysts. Although inspection of the surface is not possible with the TEM, tomography may be able to provide additional information regarding the structure and porosity of the shell. In the beam sensitive dehydrided $Ca(BH_4)_2$ material, the bubbles are found to be internal, indicating that the damage to the particle is not a chemical surface reaction.

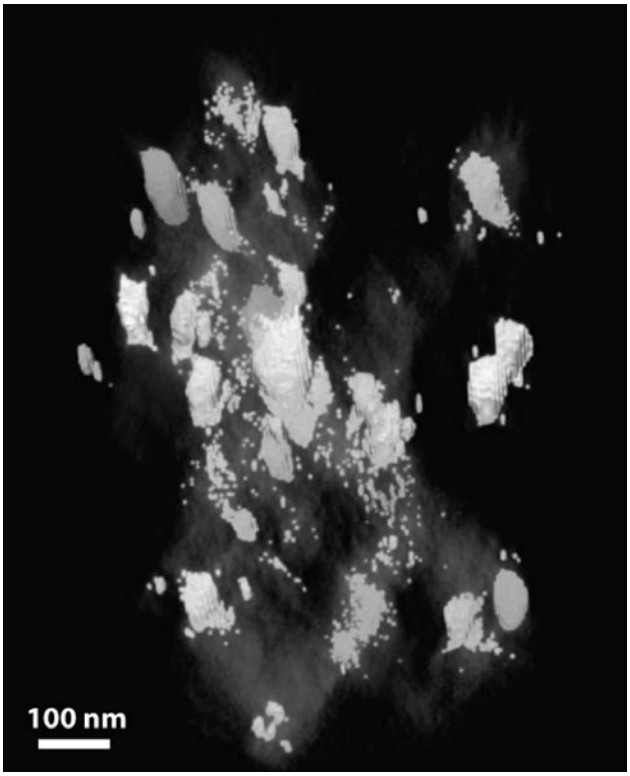

FIGURE 5. Three-dimensional tomographic reconstruction of a MgH_2 + Si + 0.05 Ni material, ball milled for five hours. The tilt angle was ±20° and the elongation factor is ~ 5x from what should be spherical particles. The Mg/Si matrix is visible as a "ghostly" scaffold underneath the opaque Ni nodules.

Aluminum-Based Systems

Ti-doped dehydrided AlH_3 + *tri*-ethyl *di*-amine (TEDA) samples obtained from Brookhaven National Laboratory have been observed in the TEM and scanning electron microscopy (SEM). In the SEM, there is no apparent segregation within the material at micron scales. The oxide layer appears to be consistent with that of Al_2O_3. On observation in the TEM, no Al/Ti segregation is seen. More notably, no surface segregation of Ti is detected (Figure 6). This indicates that Ti, as the only element present, has a catalytic effect even at low concentrations on the surface. This result may generalize to alanate systems.

Preliminary electron energy loss results on scandium-doped sodium alanate materials suggest the reduction of $ScCl_3$ does not occur until after the first cycle. The onset of the Sc $L_{2,3}$ edge in EELS will change depending on the formal charge of the Sc ion, occurring at lower energies in the reduced metallic state (Sc^0) and higher energies in the ionic Sc^{3+} form. This 3 eV shift is readily visible and provides a standardless method of determining the reduction of the doping agent inside alanate materials.

Conclusions and Future Directions

We have:

- Explored the structure and chemistry of $Ca(BH_4)_2$ and $Mg(BH_4)_2$ systems. This work is being performed in collaboration with SNL.
- Completed work on theory to address reliably the thermodynamics in molecular solids.
- Characterized the particle sizes obtained by ball milling components to introduce catalyst particles in complex hydrides.
- Demonstrated a difference in distribution of catalyst particles that depends on the catalyst.
- Matched molecular dynamics modeling results of $LiBH_4$ with experimental results on the stability of the high-temperature phase.
- Proposed possible Mg/Li alanate storage system reactions to avoid poisoning issues. This is being performed in partnership with SNL, HRL, Pitt and Georgia Tech.
- Initiated a collaboration with BNL to map the elemental distribution in Ti-doped dehydrided AlH_3.

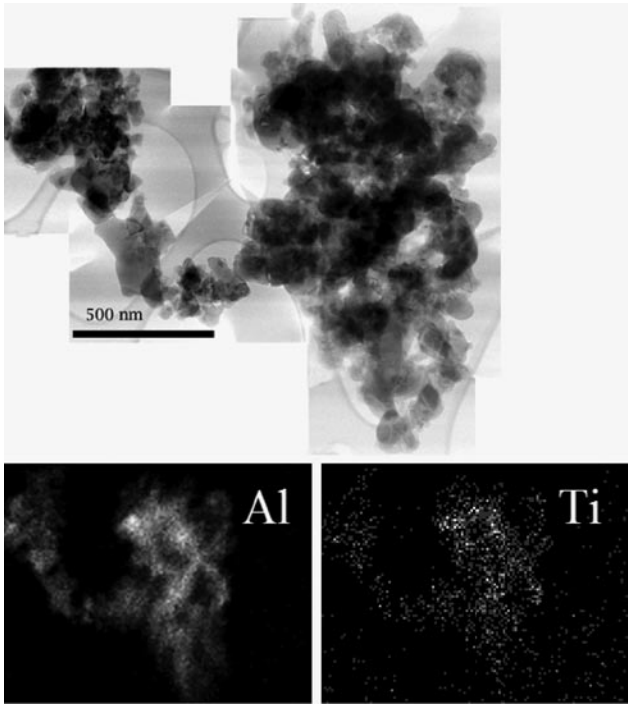

FIGURE 6. Transmission electron micrographs and X-ray chemical mapping images of dehydrided AlH_3/TEDA + 2 mol% Ti. The X-ray maps, which appear to show some variation at this scale, are actually indicative of a homogenous alloy, since greater thickness in the TEM "appears" to have higher total amounts. Over all scales measured (not all shown here), the Ti concentration is constant at 1.2 mol%. This reinforces the view that the material is very homogenous. Additionally, the Ti does not appear to be preferentially at the surface, which would appear as "coffee-stain" rings of Ti at the edges of particles in the X-ray maps.

Future directions include:

- Modeling of dodecaborane partial density of states for potential use in future EELS experiments.
- Revealing the nature of the surface coatings on catalyst particles.
- Identifying the location of $RuCl_3$ nodules within the larger $Ca(BH_4)_2$ material using tomography and energy dispersive spectroscopy. This will be compared and contrasted with particle distributions in other systems.
- Initiating surface structure studies to explore impurity effects on H_2 uptake and release, focusing initially on Al surfaces in support of MHCoE work on aluminum hydride (AlH_3).

For FY 2009 we will continue experimental studies of the microchemical and microstructural changes occurring in different candidate systems that are supplied by the various partners. Further development of the tomographic technique will yield valuable results on the positions and morphologies of catalyst particle and their distribution in the larger material.

Kinetics and poisoning issues with OH^- and O^{2+} are being addressed to try to ameliorate problems within secondary reactions within the Li-alanate to increase H_2 yield. Results of these studies may require experimental verification and we will collaborate with partners as appropriate. Additional calculations will be performed with input from partners regarding key issues.

FY 2008 Publications/Presentations

1. N.A. Zarkevich, and D.D. Johnson, "Predicting Enthalpies of Molecular Substances: exemplified via $LiBH_4$". *Physical Review Letters* 100, 040602-4 (2008).

2. N.A. Zarkevich, Teck L. Tan, L-L. Wang and D.D. Johnson, "Low-energy antiphase bound aries, degenerate superstructures, and phase stability in frustrated Ising model and Ag-Au alloys," Phys. Rev. B 77, 144208-9 (2008).

3. L.-L. Wang and D.D. Johnson, "Universal Behavior of Transition-Metal Core-Shell Nanoparticles and their Core-Shell Preference," NanoLetters, submitted 30 June 2008.

References

1. Egerton, R. F., *et al.* Ultramicroscopy, 23 (1987) 305.

2. Hwang *et al.* J Phys. Chem. C, 112 (2008) 3169.

3. Schober, T. Met. Trans. A, 12 (1981) 951.

4. Bokhonov *et al.* Mater. Letters, 5 (1987) 218.

5. Vajo, J.J. *et al.* J. Physical Chemistry B, 108 (2004) 13977.